Eurasian Chem.-Technol. J. 27 (2025) 181–190
The journal of the Institute of Combustion Problems https://ect-journal.kz

https://doi.org/10.18321/ectj1665

Thermal Decomposition and Combustion Behavior of Hydrogen Peroxide (H_2O_2) as Sustainable Fuel for Green Propulsion Technologies via Heterogeneous Low-Cost Catalysts

Hajar Jabri[1], Kainaubek Toshtay[2], Ahmed Bachar[3], Assia Mabrouk[4], Seitkhan Azat[5], Abdelaziz Sahibeddine[1], Rachid Amrousse[1]*

[1]University of Chouaib Doukkali, Faculty of Sciences, 24000 El Jadida, Morocco
[2]Department of Chemistry and Chemical Technology, Al-Farabi Kazakh National University, Almaty 050040, Kazakhstan
[3]School of Education and Training (ESEF-A), Ibnou Zohr University, Agadir 80000, Morocco
[4]Faculty of Applied Sciences, Ibnou Zohr University, Ait Melloul 80000, Morocco
[5]Institute of Mining and Metallurgical, Satbayev University, Almaty 050000, Kazakhstan

Article info

Received:
3 April 2025

Received in revised form:
26 May 2025

Accepted:
15 July 2025

Keywords:
Propellant
Specific impulse
H_2O_2
Green sustainability
Catalyst
Combustion

Abstract

Recently, hydrogen peroxide (H_2O_2) is largely used as green propellant due to its high performance, high specific impulse and low toxicity. This study investigates the catalytic performance of manganese dioxide (MnO_2) supported on silica (SiO_2) and binary silica-alumina (SiO_2-Al_2O_3) support careers for the decomposition and combustion behavior of hydrogen peroxide (H_2O_2). The primary goal is to evaluate how the addition of alumina to silica influences the catalyst's properties, particularly its textural characteristics and catalytic activity. The catalysts were thoroughly characterized using nitrogen adsorption (BET–BJH) for surface area and porosity measurements, scanning electron microscopy (SEM) coupled with energy-dispersive spectroscopy (EDS) for morphological and elemental analysis, and thermogravimetric and differential thermal analysis (DTA–TG) to assess the decomposition kinetics of H_2O_2. The results show that incorporating alumina with silica significantly enhances the dispersion of MnO_2 active phase, leading to an increase in catalytic efficiency and combustion characteristics. The SiO_2-Al_2O_3 support exhibited improved catalytic activity compared to pure silica, facilitating faster and more complete decomposition of H_2O_2. These findings suggest that optimizing the support composition can significantly improve the performance of catalysts for H_2O_2 decomposition, with potential applications in space propulsion systems where efficient, eco-friendly propellants are required.

1. Introduction

Hydrogen peroxide (H_2O_2) and hydrazine are both used as propellants in space propulsion systems, [1, 2] each with distinct advantages and disadvantages. H_2O_2 is considered a more environmentally friendly and safer alternative to hydrazine due to its decomposition into non-toxic byproducts, water, and oxygen, which significantly reduces environmental and handling risks [3-5]. This makes H_2O_2 particularly suitable for missions where safety and ecological considerations are paramount, such as small satellite propulsion and remote sensing applications [4]. Additionally, H_2O_2 is easier to store and handle compared to hydrazine, which is highly toxic and requires stringent safety measures due to its corrosive nature and potential health hazards [4, 5]. However, H_2O_2 has a lower specific impulse than hydrazine, which means it provides less thrust per unit of propellant, making it less efficient for missions requiring high propulsion efficiency, such as large space missions [4, 5]. Despite this, H_2O_2's ability to be used in both monopropellant and bipropellant systems offers flexibility in various mission scenarios [6], although its high reactivity necessi-

*Corresponding author.
E-mail address: rachid.amrousse@gmail.com

tates careful stabilization to prevent premature decomposition [4, 7]. In contrast, hydrazine's higher energy density and specific impulse make it preferable for more demanding space missions, despite its significant environmental and safety drawbacks [4, 5]. The choice between these propellants often depends on the specific requirements of the mission, balancing the need for performance with safety and environmental impact considerations [4, 5]. Overall, while Hydrogen peroxide H_2O_2 presents a promising avenue for more sustainable propulsion methodologies [8], its lower performance metrics compared to hydrazine remain a critical factor in its application [4, 5]. Catalysts play a crucial role in the decomposition reaction of H_2O_2 by significantly enhancing the reaction rate and reducing the activation energy required for the process [9]. The use of catalysts not only accelerates the decomposition but also allows for controlled energy release, which is essential for applications in propulsion systems [10]. Furthermore, the structural properties of the catalysts, such as the surface area and porosity, are critical in determining their effectiveness [11]. For instance, catalysts with higher specific surface areas, like those supported on alumina, offer more active sites, thus improving the decomposition efficiency of H_2O_2 [12, 13]. The integration of catalysts into cellular ceramics, which provide a high surface area and thermal stability, further enhances their performance in catalytic reactions, including the decomposition of H_2O_2 [14]. Overall, the role of catalysts in the decomposition of H_2O_2 is pivotal, as they not only lower the energy barrier for the reaction [15] but also improve the overall efficiency and control of the process, making them indispensable in various industrial and propulsion applications. Several catalyst types, forms, mass loadings, active phases, and supports have been developed for H_2O_2 thermal decomposition, including monolithic $MnOx/ZrO_2$ catalysts, confined tri-functional $FeOx–MnO_2/SiO_2$ catalysts, metal-foam-supported MnO_2 catalysts, bespoke nanocatalysts, and Mn_2-complex-supported nanosilica catalysts [16–20]. It is noteworthy that silica has recently been employed as a catalytic support due to its high specific surface area, which facilitates good dispersion of the active phases [21–23].

The objective of this work is to synthesize manganese-based (MnO_2) catalysts deposited on silica supports and on a 1:1 mixture of silica and alumina, and to investigate the effect of alumina addition on the efficiency of H_2O_2 decomposition. The novelty of this study lies in the synthesis of MnO_2-based particles supported on mixed alumina–silica. Silica promotes high dispersion of the active phases, while alumina provides enhanced thermal stability, as it does not transform into α-alumina below 1200 °C owing to the stabilizing (doping) effect of silica. Thus, this study aims to evaluate the catalytic performance of both catalysts in order to optimize the decomposition of H_2O_2 for space propulsion applications. Moreover, this study evaluated the catalytic reactivity of low-cost, noble-metal-free catalysts under carefully monitored laboratory conditions using a low-concentrated H_2O_2 solution (20% w/w). In addition to allowing for the evaluation of intrinsic catalytic activity without the complications of propulsion-scale environments, the use of diluted H_2O_2 ensures safe handling during preliminary screening. Before the catalyst formulations are shaped and incorporated into thruster configurations, this first stage helps to identify promising catalyst formulations. Higher concentrations of H_2O_2 and testing under typical propulsion conditions will be part of future studies. Additionally, the current strategy is in line with strict safety guidelines for catalyst development in its early stages.

2. Experimental

2.1 Catalyst Preparation

The solid heterogeneous catalysts were synthesized utilizing the superfluous solvent impregnation methodology [24-27], employing water as the solvent. The primary substance, manganese oxide, was deposited onto two separate supports: silica (SiO_2) and a 50% SiO_2 + 50% Al_2O_3 mixture as detailed in the Table 1. The γ-alumina (γ-Al_2O_3) is manufactured by Sigma Aldrich (CAS number: 1344-28-1) and the silica (SiO_2) is fabricated by Fisher Scientific (2.5–6.0 mm; product code: 12302719). The manganese concentration was fixed at 10 wt% in relation to the support. The computed quantities of precursor substances were solubilized in water and subsequently translocate into beakers. Following a maturation interval, the substrates were introduced into the beakers, and the resultant mixtures were meticulously agitated for approximately 48 h to guarantee optimal impregnation of the manganese species into the porous structures of the substrates. Subsequent to the impregnation phase, the treated specimens were positioned on a sand bath preheated to 80 °C. The specimens were sustained at this thermal condition under continuous observation with a thermometer until the solvent was entirely evaporated.

Table 1. List of catalysts, their corresponding precursors, suppliers, and product codes

Catalysts	Precursors Used	Suppliers	Codes
10% MnO_2/SiO_2 10% MnO_2/Al_2O_3-SiO_2	$NaMnO_4.H_2O$ 97%	Sigma-Aldrich	225851-250G

Consequently, the impregnated specimens were subjected to calcination at 500 °C in an ambient atmosphere utilizing a muffle furnace. The temperature was increased at a controlled rate of 5 °C/min to ensure uniform heating. This protocol facilitated the deposition and activation of manganese oxide on the substrates, thus preparing the catalysts for subsequent characterization and catalytic applications.

Catalyst Nomenclature

To simplify the identification of the synthesized catalysts, the following nomenclature has been adopted:

• **10MnSi:** Corresponds to the catalyst 10% MnO_2/SiO_2.

• **10MnSiAl:** Refers to the catalyst 10% MnO_2/Al_2O_3-SiO_2.

This nomenclature will be used throughout the article for clarity and consistency.

(i) Pre-treatment of supports:

The preliminary treatment of silica and alumina was conducted to facilitate the preparation of supports for the impregnation of the precursors. Initially, 1 g of each support material (silica and alumina) was meticulously weighed. Following this, the supports experienced calcination within a muffle furnace, adhering to a two-part temperature rise: the temperature was slowly elevated at 5 °C/min to reach 250 °C, where it remained for 2 h, and then was raised to 500 °C at the same rate, maintaining this heat for another 2 h. This calcination procedure served to activate the supports. For the silica-alumina composite, post the individual calcination of each constituent material, they were homogenously blended by grinding them together in a mortar, maintaining a 50% mass ratio for each support. This procedure ensured a uniform mixture, thereby promoting the consistent distribution of the active phase during the subsequent impregnation procedure.

(ii) Impregnation of supports:

The incorporation of the active phase MnO_2 onto the two supports pure silica (SiO_2) and a 50% SiO_2 – 50% Al_2O_3 mixture was carried out through a systematic methodology to ensure uniformity and optimal catalytic performance. The process began with the dissolution of MnO_2 precursors in distilled water, followed by continuous stirring for 2 h to achieve a homogeneous solution, preparing it for the impregnation step. In the next phase, the selected support (pure silica or the silica-alumina mixture) was added to the precursor solution. The mixture was stirred for 48 h to allow effective impregnation of MnO_2 onto the support particles, ensuring a uniform distribution of the active phase.

The impregnated samples were then dried overnight at 80 °C in an oven to remove residual water and secure the precursors onto the supports before calcination. During the final phase, the dried samples underwent calcination in a muffle furnace. The temperature was increased in two steps: first from 25 to 250 °C at a controlled rate of 5 °C/min and held for 2 h to remove water and other impurities. Then, the temperature was raised to 500 °C at the same rate and maintained for an additional 2 h. This calcination process was crucial to converting the precursors into MnO_2 and ensuring their stable deposition onto the supports. Each step was carefully monitored to guarantee homogeneous impregnation and thermal stability of the active phase, which is essential for the catalytic performance of the synthesized materials.

2.2 Catalyst Characterization

2.2.1 Morphology and Chemical Composition

The catalysts underwent characterization through the application of the Scanning Electron Microscopy – Energy Dispersive X-ray Spectroscopy (SEM-EDS) technique, aimed at elucidating their structural and compositional attributes at the nanoscale level. The metallization process was executed utilizing a DENTON VACUUM DESK V, facilitating the deposition of a thin conductive layer that is requisite for effective SEM imaging. Subsequently, high-resolution scanning electron microscopy was conducted with a HIROX SH 5500P, which yielded intricate observations regarding the surface morphology and microstructural characteristics of the catalysts. This methodological framework guaranteed an accurate and thorough characterization of the samples.

2.3 Specific Surface Area and Pore Volume

To determine the catalytic materials' specific surface area and pore volume, the N_2-adsorption technique was used, and Brunauer-Emmett-Teller (BET) and Barrett, Joyner and Halenda (BJH) analysis methods were applied in order to use it as model to calculate specific surface area and pore volume; respectively from nitrogen adsorption-desorption isotherms. These analytical techniques investigates the adsorption of nitrogen gas at cryogenic temperatures, yielding comprehensive insights into the textural characteristics of the substances, encompassing surface area and porosity. The specific surface area, pore volume, and pore size distribution of the samples were measured by N_2-physisorption at 77 K using a Micrometrics ASAP 2020. Prior to measurement, the samples were degassed under vacuum at 573 K for 4 h to clean the surfaces of the materials.

2.4 Catalyst Testing by DTA-TG Analysis

The study examined the thermal decomposition of a 20% H_2O_2 solution using both Differential Thermal Analysis (DTA) and Thermogravimetric Analysis (TGA) techniques, which also served as catalytic tests by monitoring the H_2O_2 decomposition both alone and in the presence of each catalyst [28]. A LINSEIS apparatus was used to track the process with heating rate of 10 °C/min; under air as gas vector; up to a temperature of 150 °C, ensuring complete H_2O_2 decomposition. A series of analyses were conducted by combining a drop of 5 µL of H_2O_2 with small amounts of each catalyst: 10MnSi and 10MnSiAl (about 3 mg as mass of each catalyst). This approach allowed for the investigation of the catalytic effects on H_2O_2 decomposition and facilitated a comparative analysis of the catalytic performance of both materials under uniform thermal conditions.

2.5 Combustion Characteristics

To study the behavior of H_2O_2 solutions, a series of burning tests were conducted at elevated pressures using a strand burner device housed within a pressure vessel. The open-button strand burner was positioned at the center of the vessel, and a glass tube preloaded with H_2O_2 solution and H_2O_2 with MnO_2 catalytic particles as additives (i.e. same preparation method of 10% MnO_2/Al_2O_3-SiO_2), and equipped with a wire was placed inside [29]. Following ignition and combustion, the resulting gases were vented from the vessel. An electrical feedthrough was used to supply the energy required for ignition. The vessel included a pressure regulator to monitor static pressure, as well as optical windows to allow light access. High-speed motion recordings were captured using high-speed camera, operating at 500 frames per second (fps), and capable of reaching up to around 2000 fps. In a typical test, the strand burner with the prefilled H_2O_2-containing glass tube was placed inside the vessel, which was then pressurized with nitrogen. Propellant ignition was achieved via an electrical discharge. After the combustion test, the vessel was depressurized, opened, cleaned, and prepared for the next experiment. To determine the burning rate, short image intervals were extracted from the recorded videos. The Image J software was then used to analyze the change in liquid surface area over time.

3. Results and Discussion

3.1 Characterization of Support Careers and Catalysts

3.1.1 Morphology of Prepared Samples

The prepared samples were first characterized using SEM-EDS analysis. The resulting micrographs and corresponding EDS spectra for the 10MnSi and 10MnSiAl catalysts are shown in Figs. 1 and 2, and summarized in Tables 2 and 3, respectively.

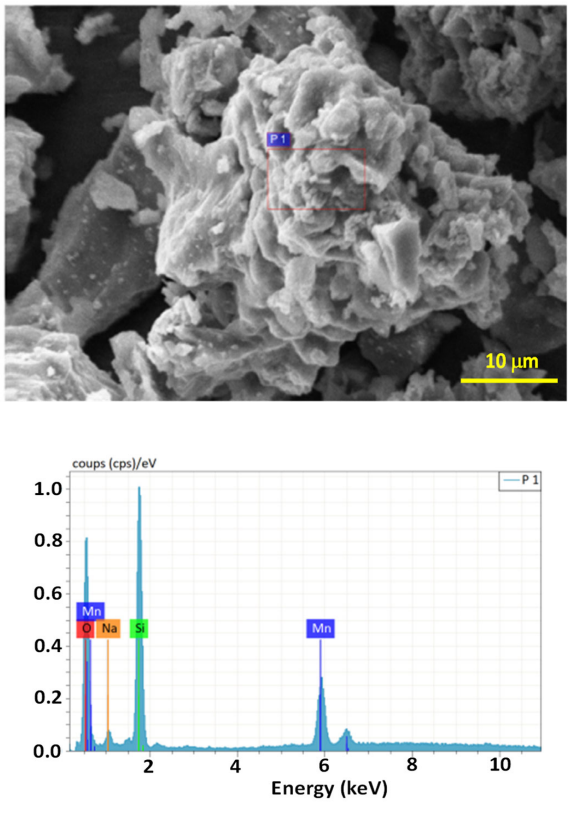

Fig. 1. SEM micrograph and EDS spectrum of the 10MnSi catalyst.

Table 2. EDS elemental composition of the 10MnSi catalyst

Element	A	Net	Mass [%]	Atom [%]
Oxygen	8	15584	26.04	54.13
Sodium	11	1168	2.62	3.79
Silicon	14	24647	30.48	36.10
Manganese	25	9199	9.87	5.98
		Total:	69.01	100.00

SEM analysis reveals a granular morphology with uniformly dispersed MnO_2 particles embedded within the SiO_2 matrix, maximizing the active surface area for catalytic interactions. EDS analysis confirms the compositional characteristics, with silicon (44.47%) and oxygen (37.73%) as the principal components of the SiO_2 matrix. Manganese (9.87%) aligns closely with the expected MnO_2 ratio, ensuring optimal catalytic efficiency. The detected sodium content (3.79%) originates from the use of sodium permanganate as a precursor during the synthesis process and is unlikely to significantly affect the material's performance. These results validate the material's suitability for efficient and controlled H_2O_2 decomposition.

3.1.3 10MnSiAl Catalyst

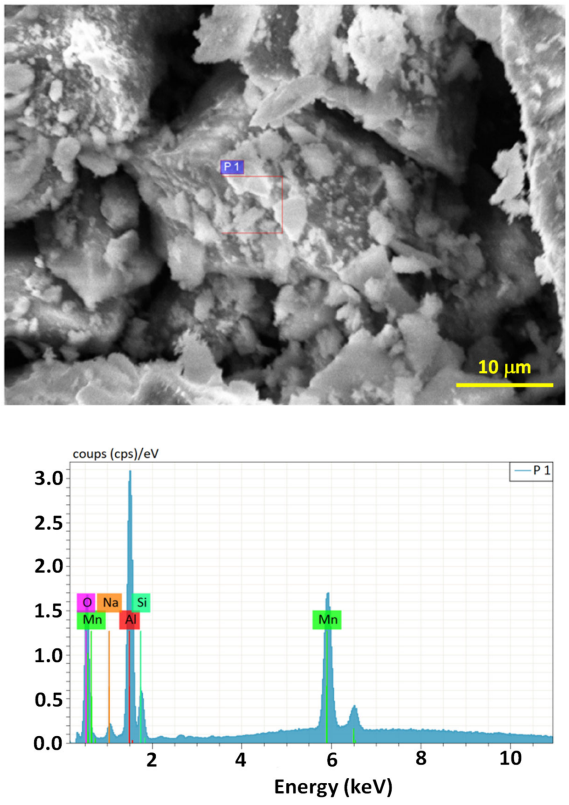

Fig. 2. SEM micrograph and EDS spectrum of the 10MnSiAl catalyst.

Table 3. EDS elemental composition of the 10MnSiAl catalyst

Element	A	Net	Mass [%]	Atomic [%]
Oxygen	8	30.950	10.45	30.03
Sodium	11	2.888	1.60	3.21
Aluminium	13	71.414	26.81	45.68
Silicon	14	13.687	6.83	11.18
Manganese	25	60.809	11.83	9.90
Total			57.53	100.00

In the analysis performed using scanning electron microscopy (SEM), the catalyst composed of 10MnSiAl exhibits a complex and well-defined morphology, indicating a homogeneous integration of MnO_2 into the silica-alumina matrix. Energy-dispersive spectroscopy (EDS) confirms the chemical composition, highlighting aluminum (46.06%) and silicon (24.18%) as the predominant elements within the matrix, while oxygen (18.17%) supports the oxide structure. The manganese content (11.83%) aligns accurately with the intended 10% MnO_2 ratio, ensuring an optimal distribution of active catalytic sites for the decomposition of hydrogen peroxide (H_2O_2). The detected sodium content (2.79%) is attributed to the use of sodium permanganate as a precursor during synthesis; however, this low concentration has no significant impact on the catalytic performance of the material. These findings demonstrate a well-engineered catalyst characterized by controlled manganese incorporation and a stable oxide matrix, providing high efficiency and controlled performance for the decomposition of H_2O_2 in space propulsion applications.

3.1.4 Textural Properties

The results of N_2-sorption using BET and BJH analysis methods pertaining to the catalysts are encapsulated in the subsequent Table 4.

Table 4. Textural properties of catalysts: S_{BET} (specific surface area) and V_p (pore volume)

Catalysts	S_{BET} (m^2/g)	V_p (cm^3/g)
10MnSi	0.8	0.002
10MnSiAl	81	0.15

The results of the BET and BJH analysis methods indicate a pronounced disparity in the textural characteristics between the two catalysts under examination. The 10MnSi catalyst demonstrates

an exceedingly low total specific surface area (S_{BET} = 0.8 m^2/g), characterized by a relatively equitable distribution between microporous surface area and external surface area, accompanied by a markedly restricted pore volume (V_p = 0.002 cm^3/g). These metrics imply a poorly developed structural framework with minimal porosity, which may impede the accessibility of active sites and, as a result, diminish catalytic efficacy. Conversely, the introduction of alumina into the 10MnSiAl catalyst substantially ameliorates the textural attributes of the material. The total specific surface area escalates to 81 m^2/g, signifying a dramatic enhancement in comparison to 10MnSi. This advancement is predominantly attributable to the augmentation of external surface area, whereas the microporous surface area remains comparatively modest. The overall pore volume (V_p = 0.15 cm^3/g) further substantiates a significantly more developed porosity. These results imply that introducing alumina aids in creating a more open porous framework, which may improve the diffusion of reactants and strengthen the catalytic effectiveness of the substance, especially in reactions with bigger molecules.

3.2 DTA-TG Analysis

This investigation centered on the thermal decomposition approach of a 20% (w/w) hydrogen peroxide solution, employing differential thermal analysis and thermogravimetric analysis (DTA-TGA) apparatus. The experiments were carried out under four unique conditions: devoid of a catalyst, in conjunction with three MnO_2-based catalysts anchored on SiO_2, Al_2O_3, and a composite of both support substrates. These investigations sought to assess the effectiveness of each catalytic configuration in facilitating the decomposition process, thereby elucidating the effect of the support material on catalytic efficacy. The findings underscore the comparative performance of the evaluated systems and presented in the Fig. 3.

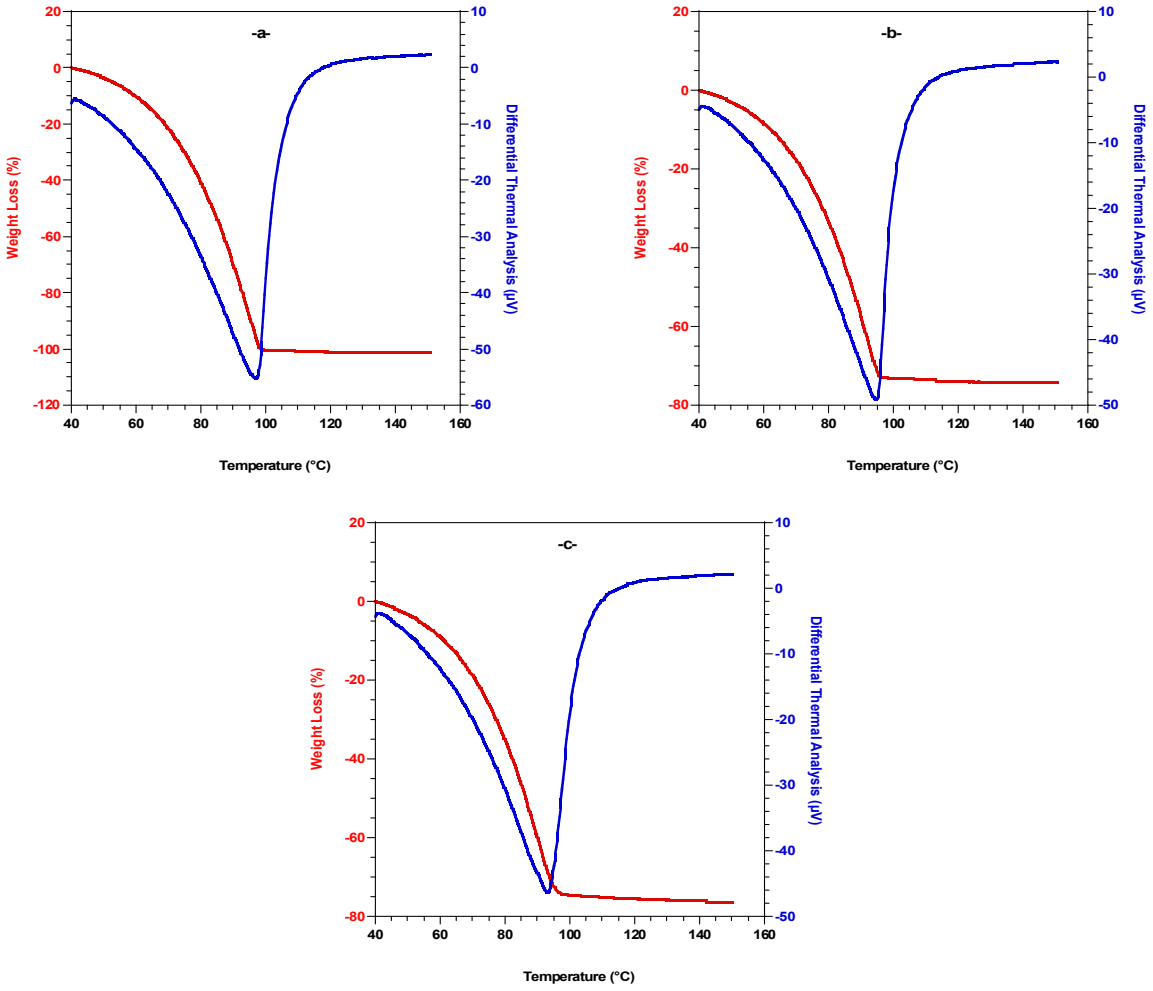

Fig. 3. DTA-TGA thermograms of the thermal decomposition of 20% (w/w) H_2O_2: (a) H_2O_2 without catalyst; (b) H_2O_2 with 10MnSi catalyst; (c) H_2O_2 with 10MnSiAl catalyst.

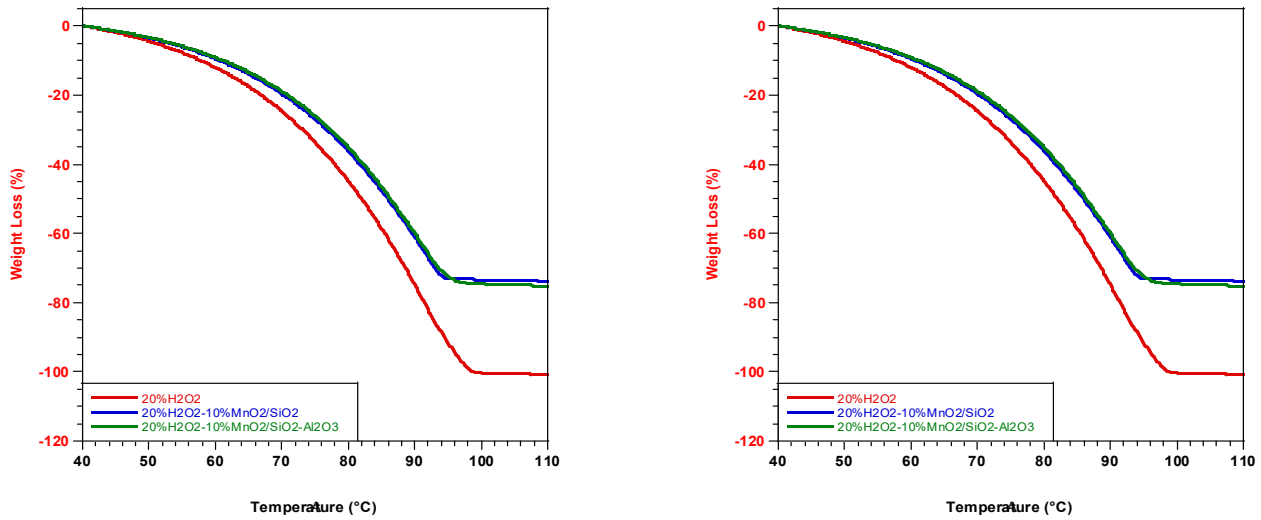

Fig. 4. Comparative data on the DTA-TGA thermograms of the thermal decomposition of 20% (w/w) H_2O_2 alone (without catalyst) and in the presence of 10MnSi and 10MnSiAl catalysts.

In the scenario pertaining to H_2O_2 in isolation (graph a), the phenomenon observed is predominantly thermal evaporation, which is characterized by a gradual diminution of mass up to approximately 80 °C, succeeded by an acceleration in mass loss between 80 and 100 °C, devoid of any discernible exothermic peak evident in the DTA curve. The addition of the 10MnSi catalyst (Fig. 3b) does not substantially alter the observed behavior, primarily due to its limited activity at low temperatures. The high water content (80%) further restricts catalytic performance in this region, with activity becoming evident only at elevated temperatures, as confirmed by the completion of evaporation near 100 °C. In contrast, the 10MnSiAl catalyst promotes earlier evaporation, which is completed at approximately 90 °C. These findings highlight the potential of 10MnSi as a candidate for propulsion applications, attributable to its ability to enhance oxygen release and thermal energy generation. The catalytic effect is further intensified with the 10MnSiAl catalyst (Fig. 3c), as evidenced by a pronounced mass loss at reduced temperatures, indicative of a rapid and efficient decomposition process. A magnified analysis additionally reveals a progressive mass loss beginning near 40 °C, which may correspond to the onset of decomposition or the release of volatile species. These observations elucidate that the 10MnSiAl catalyst further reduces the decomposition temperature and significantly enhances the reaction kinetics, thereby affirming its substantial potential for catalytic applications within the domain of propulsion.

As compared in the Fig. 4, the examination of the DTA-TGA thermograms reveals that, in addition to accelerating the decomposition of hydrogen peroxide, the 10MnSi and 10MnSiAl catalysts also enhance its thermal stability. TGA results indicate that, unlike the abrupt mass loss observed for pure H_2O_2, the incorporation of these catalysts mitigates this loss, suggesting a more controlled reaction pathway. Moreover, the DTA profile of pure H_2O_2 exhibits a pronounced endothermic peak, indicative of significant heat absorption, whereas the addition of the catalysts reduces both the intensity and the onset temperature of this peak, confirming the facilitated decomposition process. The enhanced performance of the 10MnSiAl catalyst could be attributed to the presence of Al_2O_3, which may promote the dispersion of MnO_2 or stabilize reactive intermediates. These effects are particularly relevant for applications requiring stringent thermal control, such as propulsion systems or chemical processes involving controlled oxygen release.

3.3 Combustion Behavior

The combustion behavior of 20 wt.% H_2O_2 was investigated both in its pure form and with the addition of MnO_2 catalytic particles (8–10 mg catalyst loading) deposited on alumina-silica (MnO_2/AlSi) using a strand burner at ambient temperature under varying pressure conditions, as illustrated in Fig. 5a. Figure 5b shows an example of bubble formation during the H_2O_2 combustion in the presence of the MnO_2 catalyst.

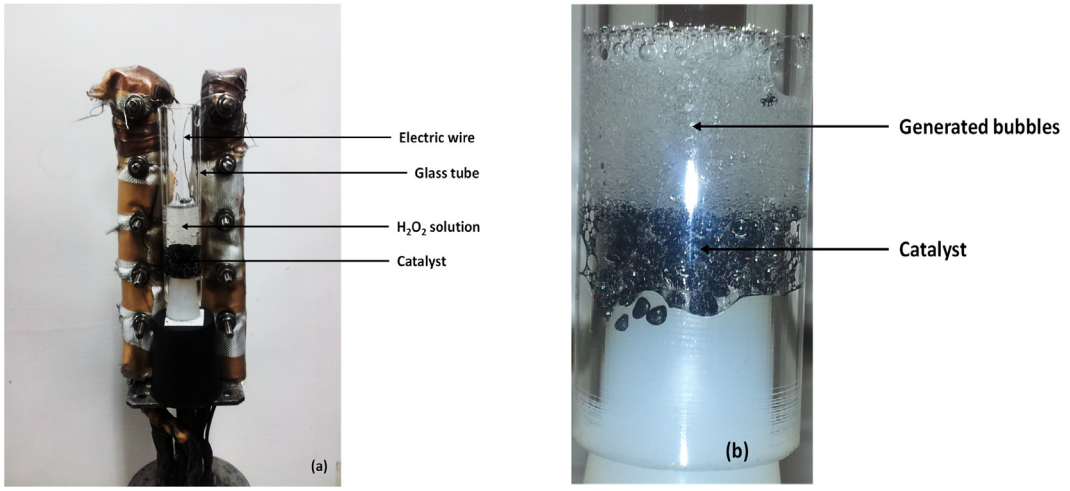

Fig. 5. (a) Glass tube filled with H_2O_2 solution for combustion experiment and (b) generated bubbles of H_2O_2 combustion in the presence of MnO_2/AlSi catalyst.

Using high-speed video motions that were analyzed to determine the burning rates. The obtained data were presented in the Fig. 6. In fact, the burning rates were calculated using the formula:

$$r_b = \frac{S}{t}$$

where r_b is the burning rate in mm/s^2, S(mm^2) is the surface of cylindrical glass tube, and t(s) the time of the burned solution totally.

Figure 6 illustrates the relationship between pressure and the burning rate of hydrogen peroxide, highlighting the catalytic effect of MnO_2 particles. At low pressures, the burning rates remain quite low, and the addition of MnO_2 catalyst shows minimal to no impact. This suggests that under such conditions, the combustion process is limited, likely due to insufficient reaction intensity or bubble formation. As pressure increases, a noticeable rise in burning rates is observed, indicating that higher pressure enhances the decomposition and combustion processes. Most importantly, the presence of MnO_2 particles becomes significantly impactful at these elevated pressures. The burning rate increases much more sharply with the catalyst, implying an enhanced reaction mechanism. This behavior can be explained by the nature of bubble formation during decomposition. At high pressures, larger bubbles are generated. These larger bubbles are more prone to rupture under the influence of catalytic particles, which accelerates the breakdown of hydrogen peroxide and boosts the release of oxygen and heat, increasing the burning rate. In summary, MnO_2/AlSi particles act as effective catalysts at high pressures, enhancing the combustion of H_2O_2. Their impact is limited at low pressures but becomes significantly beneficial as

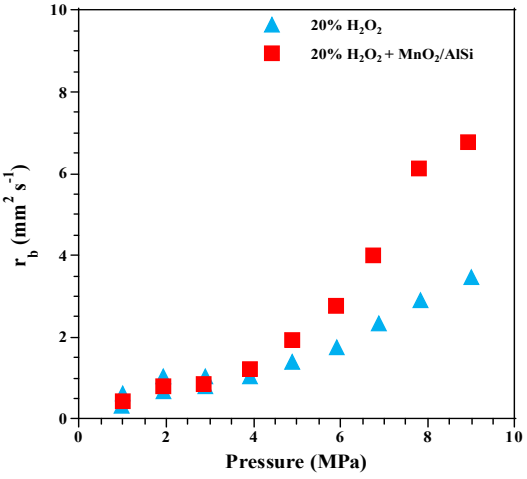

Fig. 6. The measured burning rates of H_2O_2 combustion of 20 wt.% H_2O_2 alone and 20 wt.% H_2O_2 with MnO_2/AlSi catalytic particles as additives.

pressure rises, due to their role in promoting bubble breakup and accelerating the reaction kinetics.

This study aimed to evaluate the catalytic performance of low-cost, noble-metal-free MnO_2/AlSi-based catalysts supported on silica and alumina-silica matrices for the decomposition of low-concentrated 20 wt.% H_2O_2, with potential application as a green propellant, as previously discussed [30]. The catalytic influence was initially assessed through thermal analysis using differential thermal analysis and thermogravimetric analysis (DTA-TG), enabling a comparative investigation of H_2O_2 decomposition behavior in the absence and presence of catalytic particles. The incorporation of MnO_2/AlSi-based catalysts resulted in a noticeable enhancement in the thermal decomposition profile of H_2O_2, indicating a significant reduction in the activation energy and a shift in the decomposition temperature. To complement the

thermal data, the combustion characteristics of H_2O_2 were examined by measuring burning rates as a function of pressure, both with and without the presence of the catalytic materials. The results demonstrated that MnO_2/AlSi catalysts not only promoted faster decomposition but also improved the combustion stability and energy release efficiency. Finally, textural and morphological analyses of the synthesized catalysts were conducted. Nitrogen adsorption-desorption isotherms were recorded to determine surface area and pore structure via the BET and BJH analysis methods, SEM-EDS was used to assess the morphology and elemental distribution of the catalysts. The comprehensive analysis confirms the potential of MnO_2/Al-Si-based systems as effective and economically viable catalysts for green propulsion applications.

4. Conclusion

The primary objective of this study was to assess the catalytic efficacy of manganese dioxide (MnO_2)-based materials supported on silica (10MnSi) and a silica–alumina mixture (10MnSiAl) for the decomposition of hydrogen peroxide (H_2O_2), with promising potential for applications in environmentally sustainable propulsion systems. Thermal analytical methods (DTA-TGA) demonstrated a marked enhancement in the decomposition of H_2O_2 in the presence of both catalytic materials. The 10MnSiAl catalyst exhibited a more rapid and exothermic decomposition at lower temperatures, indicating superior catalytic activity. This performance highlights its suitability for systems requiring swift and regulated oxygen release, particularly in space propulsion.

We found also how pressure affects the burning rate of H_2O_2, especially in the presence of MnO_2 as a catalyst. At low pressures, the burning rate remains low and MnO_2 has little effect, likely due to weak reaction intensity or limited bubble formation. As pressure increases, the burning rate rises significantly, and the catalytic effect of MnO_2 becomes much more pronounced. This is attributed to the formation of larger bubbles that rupture more easily in the presence of the catalyst, enhancing the decomposition process. Overall, MnO_2/AlSi is effective in boosting H_2O_2 combustion at high pressures by accelerating reaction kinetics through better bubble breakdown. The N_2-sorption by BET and BJH analysis methods corroborated these findings, showing that 10MnSiAl possesses a significantly higher specific surface area (~81 m^2/g) and greater pore volume compared to 10MnSi. These improved textural characteristics enhance accessibility to active sites, thereby improving catalytic performance. SEM-EDS further supported these results. The 10MnSi catalyst exhibited a uniform granular morphology with well-dispersed MnO_2 particles within the silica matrix, ensuring effective active site distribution. In contrast, 10MnSiAl showed a more complex and well-defined structure, with homogeneous MnO_2 integration into the silica-alumina matrix, confirming its structural integrity. EDS confirmed the expected chemical composition, with a manganese content close to 10% and low sodium levels -residual from the precursor – that do not significantly affect catalytic performance.

In conclusion, the incorporation of alumina markedly improves the structural properties, thermal stability, and dispersion of MnO_2, positioning the 10MnSiAl catalyst as a highly promising candidate for processes requiring efficient, rapid, and controlled H_2O_2 decomposition, especially within the framework of green propulsion technologies.

References

[1]. F.F. Maia, L.H. Gouvea, L.G.F. Pereira, et al., Development and optimization of a catalytic thruster for hydrogen peroxide decomposition, *J. Aerosp. Technol. Manag.* 6 (2014) 61–67. DOI: 10.5028/jatm.v6i1.286

[2]. I. Remissa, H. Jabri, Y. Hairch, et al., Propulsion Systems, Propellants, Green Propulsion Subsystems and their Applications: A Review, *Eurasian Chem.-Technol. J.* 25 (2023) 3–19. DOI: 10.18321/ectj1491

[3]. B. Martin, J. Sedelmeier, A. Bouisseau, et al., Toolbox study for application of hydrogen peroxide as a versatile, safe and industrially-relevant green oxidant in continuous flow mode, *Green Chem.* 19 (2017) 1439–1448. DOI: 10.1039/c6gc02899c

[4]. H. Jabri, A. Sahibeddine, R. Amrousse, "Hydrogen Peroxide (H2O2) Decomposition as Green Propellant: Overview of Synthesized Catalysts." Innovative Materials for Environmental and Aerospace Applications, edited by Rachid Amrousse, et al., IGI Global Scientific Publishing, 2025, pp. 247-278. DOI: 10.4018/979-8-3373-0669-8.ch007

[5]. A. Souagh, I. Remissa, R. Amrousse, Catalytic materials for space propulsion applications, in: Advances in Chemical and Materials Engineering Book Series, 2024: pp. 279–326. DOI: 10.4018/979-8-3373-0669-8.ch008

[6]. R. Amri, D. Gibbon, T. Rezoug, The design, development and test of one newton hydrogen peroxide monopropellant thruster, *Aerosp. Sci. Technol*. 25 (2012) 266–272. DOI: 10.1016/j.ast.2012.02.002

[7]. D. Sengupta, S. Mazumder, J.V. Cole, S.A. Lowry, Controlling Non-Catalytic Decomposition of High-Concentration Hydrogen Peroxide. U.S. Department

of Defense Technical Report, 2004. DOI: 10.21236/ada426795

[8]. Y. Tian, D. Deng, L. Xu, et al., Strategies for sustainable production of hydrogen peroxide via oxygen reduction reaction: from catalyst design to device setup, *Nano-Micro Lett.* 15 (2023). DOI: 10.1007/s40820-023-01067-9

[9]. P. Pędziwiatr, F. Mikołajczyk, D. Zawadzki, et al., Decomposition of hydrogen peroxide - kinetics and review of chosen catalysts, *Acta Innovations* (2018) 45–52. DOI: 10.32933/actainnovations.26.5

[10]. R. Amrousse, A.N. Elidrissi, A. Bachar, et al. "Nanosized Catalytic Particles for the Decomposition of Green Propellants as Substitute for Hydrazine: Application of Catalysis and Nanocatalysis in Green Propulsion." Innovations and Applications of Hybrid Nanomaterials, edited by Virat Khanna, et al., IGI Global Scientific Publishing, 2024, pp. 195-217. DOI: 10.4018/979-8-3693-3268-9.ch009

[11]. G. Palmisano, S.A. Jitan, C. Garlisi, Surface area and porosity, in: Elsevier eBooks, 2022: pp. 101–140. DOI: 10.1016/b978-0-323-89845-4.00003-5

[12]. N.-A.M. Deraz, M.A. El-Sayed, A.Abd. El-Aal, Catalytic Decomposition of H_2O_2 over Manganese Oxides Supported on an Active Alumina, *Adsorpt. Sci. Technol.* 19 (2001) 541–551. DOI: 10.1260/0263617011494385

[13]. Z. Harimech, M. Salah, R. Amrousse, Ammonium dinitramide (ADN) decomposition as Green propellant, in: Advances in Chemical and Materials Engineering Book Series, 2024: pp. 169–194. DOI: 10.4018/979-8-3693-7505-1.ch006

[14]. Y. Hairch, A.E.S. Nosseir, M. Atamanov, R. Amrousse, Cellular ceramics used as catalytic supports for heterogeneous catalyst synthesis, in: Advances in Chemical and Materials Engineering Book Series, 2024: pp. 1–38. DOI: 10.4018/979-8-3693-7505-1.ch001

[15]. L. Micoli, G. Bagnasco, M. Turco, et al., Vapour phase H_2O_2 decomposition on Mn based monolithic catalysts synthesized by innovative procedures, *Appl. Catal. B: Environ*. 140–141 (2013) 516–522. DOI: 10.1016/j.apcatb.2013.04.072

[16]. L. Micoli, M. Turco, Decomposition of H_2O_2 on Monolithic MnOx/ZrO_2 Catalysts for Aerospace Application, *Chem. Eng. Trans.* 43 (2015) 1819–1824. DOI: 10.3303/CET1543304

[17]. Y. Yang, L. Shi, J. Lin, et al., Confined Tri-Functional FeO_x@MnO_2@SiO_2 Flask Micromotors for Long-Lasting Motion and Catalytic Reactions, *Small* 19 (2023). DOI: 10.1002/smll.202207666

[18]. P. Surmacz, Z. Gut, The experimental investigation of a 98% hydrogen peroxide monopropellant thruster comprising the Metal-Foam-Supported manganese oxide catalyst, *Aerospace* 10 (2023) 215. DOI: 10.3390/aerospace10030215

[19]. Sherif Elbasuney, Mohamed Attwa, A. Deif et al. Green Synthesis and Catalytic Activity Assessment of Bespoke Nano- Catalyst for Eco-Friendly Green Propellant Systems based on Hydrogen Peroxide, 15 December 2022, PREPRINT available at Research Square. DOI: 10.21203/rs.3.rs-2366759/v1

[20]. T. Pelluau, S. Sene, B. Garcia-Cirera, et al., Multifunctionalized Mesostructured Silica Nanoparticles Containing Mn2 Complex for Improved Catalase-Mimicking Activity in Water, *Nanomaterials* 12 (2022) 1136. DOI: 10.3390/nano12071136

[21]. M. Timusk, A. Kuus, K. Utt, et al., Thick Silica Foam Films through Combined Catalytic Decomposition of H_2O_2 and Sol-Gel Processes, *Mater. Des.* 111 (2016) 80–87. DOI: 10.1016/j.matdes.2016.08.092

[22]. A.L.-T. Pham, C. Lee, F.M. Doyle, D.L. Sedlak, A Silica-Supported iron oxide catalyst capable of activating hydrogen peroxide at neutral pH values, *Environ. Sci. Technol.* 43 (2009) 8930–8935. DOI: 10.1021/es902296k

[23]. R. Javaid, U.Y. Qazi, S.-I. Kawasaki, Efficient and Continuous Decomposition of Hydrogen Peroxide Using a Silica Capillary Coated with a Thin Palladium or Platinum Layer, *Bull. Chem. Soc. Jpn.* 88 (2015) 976–980. DOI: 10.1246/bcsj.20150052

[24]. N.M. Deraz, The comparative jurisprudence of catalysts preparation methods: I. Precipitation and impregnation methods, *Journal of Industrial and Environmental Chemistry* 1 (2017) 25–27.

[25]. C. Perego, P. Villa, Catalyst preparation methods, *Catal. Today* 34 (1997) 281–305. DOI: 10.1016/s0920-5861(96)00055-7

[26]. M.V. Twigg, Catalyst Handbook, 2018. DOI: 10.1201/9781315138862

[27]. G. Ertl, H. Knözinger, F. Schüth, J. Weitkamp (Eds.), Handbook of Heterogeneous Catalysis, 8-volume set, Wiley-VCH, Weinheim, 2008. DOI: 10.1002/9783527610044

[28]. I. Remissa, A. Souagh, Y. Hairch, et. al., Thermal decomposition behaviors of 30% hydrogen peroxide over free noble metal-synthesized solid catalysts, *Int. J. Energ. Mat. Chem. Propul.* 21 (2022) 17. DOI: 10.1615/IntJEnergeticMaterialsChemProp.2022043338

[29]. R. Amrousse, T. Katsumi, N. Azuma, K. Hori, Hydroxylammonium nitrate (HAN)-based green propellant as alternative energy resource for potential hydrazine substitution: From lab scale to pilot plant scale-up, *Combust. Flame* 176 (2017) 334-348. DOI: 10.1016/j.combustflame.2016.11.011

[30]. Y. Kasbi, I. Remissa, K. Toshtay, et al., H_2O_2 and HAN green monopropellants: a state-of-the-art review on their recent development, corresponding synthesized catalysts, and their possible use as thrusters, *Catalysts* 15 (2025) 183. DOI: 10.3390/catal15020183